Virology 384 (2009) 151–160

Contents lists available at ScienceDirect

Virology

journal homepage: www.elsevier.com/locate/yviro

The role of the cowpox virus crmA gene during intratracheal and intradermal infection of C57BL/6 mice

A.L. MacNeill [a,*], L.L Moldawer [b], R.W. Moyer [c]

[a] University of Illinois College of Veterinary Medicine, Department of Pathobiology, 2001 S. Lincoln Ave., Urbana, IL 61802, USA
[b] University of Florida College of Medicine, Department of Surgery, P.O. Box 100286, Gainesville, FL 32610, USA
[c] University of Florida College of Medicine, Department of Molecular Genetics and Microbiology, P.O. Box 100226, Gainesville, FL 32610, USA

ARTICLE INFO

Article history:
Received 25 August 2008
Return to author for revision
24 September 2008
Accepted 29 October 2008
Available online 4 December 2008

Keywords:
Poxvirus
Cowpox virus
Intratracheal inoculation
Intradermal inoculation
Pathogenesis
crmA
Pneumonia
Mouse model of smallpox
Virulence factor
Attenuation of cowpox virus

ABSTRACT

Intratracheal (i.t.) infection of mice with cowpox virus (CPXV), is lethal at a lower dose than intranasal (i.n.) inoculation. CPXV deleted for cytokine response modifier A (CPXVΔcrmA) was attenuated compared to CPXV after i.t. inoculation. This attenuation could not be attributed to differences in virus replication, immunomodulators, or cells infiltrating the lungs. Deletion of crmA also caused attenuation during intradermal (i.d.) infection. In contrast to i.t.-inoculated virus, deletion of crmA reduced virus replication at the site of infection. This difference correlated to increased numbers of $CD3^+$ cells in CPXVΔcrmA-associated dermal lesions. Thus, crmA is a virulence factor in mice during either pulmonary or dermal cowpox infection; however the influence of crmA is more evident during i.d. inoculation. This suggests that the host immune response differs in the two routes of infection and emphasizes the need to consider the effect of route of infection when examining functions of virulence factors *in vivo*.

Introduction

Smallpox is a dreaded, often fatal, human viral disease hallmarked by severe skin lesions and pneumonia (Fenner, 1984). A similar disease is caused by monkeypox virus, which is indigenous in equatorial Africa. Although smallpox has been eradicated through extensive vaccination of the human population, there is strong interest in improving current animal models of smallpox infection. In this manner, the disease can be studied indirectly and new control methods developed in the event that the causative agent of smallpox (variola virus) is released into the environment (Ferrier-Rembert et al., 2007) or to control emerging human monkeypox virus infections. Due to the human-specific nature of variola virus, other related Orthopoxviruses, such as zoonotic cowpox virus (CPXV), have been utilized as surrogate model viruses. Since rodents (particularly voles and woodmice) are thought to be reservoir hosts of CPXV (Chantrey et al., 1999), mice infected with CPXV have been used to evaluate host/pathogen interactions. Mouse models are clearly advantageous because of the excellent characterization of most mouse strains, the availability of transgenic mice and a variety of mouse-specific immunologic reagents, and their relatively inexpensive maintenance.

A natural infection by CPXV typically results from introduction of virus into the skin and usually produces mild disease unless the host is immunosuppressed. Variola virus is typically introduced via aerosolized particles or dermal inoculation. In human dermal infections, there is approximately a seven day incubation period after exposure to CPXV or variola virus before fever and flu-like symptoms begin (Breman and Henderson, 2002; Lewis-Jones, 2004). In both cowpox and smallpox infections, papules that form in the skin at the site of inoculation develop into black eschars surrounded by edema and erythema. The lesions become covered by scabs which then shed leaving a scar. In the case of variola virus, virus particles commonly spread throughout the body. Replication of variola virus in the lung leads to severe pneumonia and difficulty with oxygenation and ventilation. Respiratory compromise, along with dehydration due to fluid loss through breaks in the skin (leading to shock and renal failure), are the most likely causes of death in smallpox victims (Martin, 2002). In contrast, CPXV replication in humans is usually limited to skin lesions at the site of introduction. However, there are rare cases of human CPXV infection, where virus from the initial site of infection in the skin spreads to and replicates in the lungs, resulting in mortality due to complications of viral pneumonia (Hawranek et al.,

* Corresponding author. Fax: +1 217 244 7421.
E-mail address: almac@illinois.edu (A.L. MacNeill).

0042-6822/$ – see front matter © 2008 Elsevier Inc. All rights reserved.
doi:10.1016/j.virol.2008.10.041

2003). Moreover, viremia has been detected in humans after being naturally infected with CPXV (Nitsche et al., 2007).

Typically, experimental infection of mice with CPXV has been designed to result in the afflicted animals exhibiting signs of systemic disease and experiencing pneumonia; conditions similar to those caused by variola virus in humans. To produce such pulmonary disease in immunocompetent mice, large doses of CPXV are administered directly to their respiratory system by aerosolized or intranasal (i.n.) inoculation. Although aerosolization is usually effective (Martinez et al., 2000), there are inherent problems with the procedure including the need for specialized equipment that enables adequate suspension of the virus, a required size of the aerosolized particles for efficient uptake by the mice, and the potential for environmental contamination with the virus. While the practice of i.n. inoculation avoids the concerns associated with virus aerosolization, the desired outcome of pulmonary disease is not always achieved. Instead, in the study by Martinez et al. (2000), only half of the mice infected i.n. developed pulmonary disease, but all of the mice had severe rhinitis and sinusitis (which likely contributed to death). Moreover, as with application of aerosolized virus, exact dosage of the pathogen is difficult to achieve during i.n. exposure due to variable reflux, expulsion, and loss of the inoculum to the overall surroundings and immediate external area (fur) of the treated animal.

In addressing the need for a reliable representation of smallpox in mice, we decided to evaluate intratracheal (i.t.) inoculation as a novel method for poxvirus introduction into this animal. This approach ensures that a more precise number of viral particles are distributed throughout the lower respiratory tract by bypassing the nasal and oral cavities and avoids the technical difficulties associated with aerosol and i.n. inoculations. We chose to infect C57BL/6 mice in lieu of the BALB/c strain traditionally used to examine poxvirus pathogenesis because of differences in important facets of their immune systems. Specifically, the latter does not mount strong cell-mediated immune responses against viral infection (Janeway et al., 1999) and has a less active complement system due to lower production of the complement protein C3 (Dieli et al., 1988). In addition, future studies would benefit from utilizing C57BL/6 mice as this strain is more commonly used as a progenitor for commercially available transgenic mice.

We also performed a comparative assessment of the disease which resulted from intradermal (i.d.) inoculation of mice via the ear pinnae; a method first described by Tscharke et al. (2002). Intradermal infections more closely mimic the typical natural route of CPXV transmission and dermal models of poxvirus infection have been implemented to test the effectiveness of smallpox vaccines (Melamed et al., 2007). Both i.t. and i.d. models utilize natural routes of poxvirus infection (into the lung or skin respectively), but i.d. infection of mice with CPXV fails to produce the severe pulmonary infection reported after i.d. inoculation of humans with variola virus. In experiments with the closely related Orthopoxvirus, vaccinia virus (VACV), it appears that there are marked differences in the immune response to i.d. inoculation of mice compared to the response following i.n. inoculation (Tscharke et al., 2002). We sought to determine if this also was the case with CPXV infection and we have compared the pathogenesis of CPXV infection after i.d. inoculation to the i.t. model.

We also compared wild type (wt) CPXV and a mutant of CPXV which lacked the gene encoding cytokine response modifier A (crmA) referred to as CPXVΔcrmA (Nathaniel et al., 2004). The crmA protein is a *ser*ine *p*roteinase *in*hibitor (serpin) that inhibits the serine proteinase granzyme B (Quan et al., 1995) as well as group 1 and 3 cysteine aspartyl-specific proteinases (caspases) (Garcia-Calvo et al., 1998). Thus, *in vivo*, crmA complex formation with caspase-1 may prevent the processing of soluble interleukin-1β (IL-1β) and IL-18; absence of these mediators would lead to decreased inflammation at the site of infection and reduce activation of cell-mediated cytotoxicity. Furthermore, the predicted crmA inhibition of granzyme B, caspase-8, -9, and -10 activity would limit apoptosis of virus-infected cells and hence, enable more efficient replication of the virus.

The crmA gene is highly conserved in a variety of other poxviruses (Smith et al., 1989) and in VACV is referred to as 'SPI-2' or B13R. Although the importance of crmA expression during CPXV infection has not been established in immunocompetent animals, this protein has been demonstrated to be a virulence factor when CPXV was grown in the chorioallantoic membranes of developing chicken embryos where CPXVΔcrmA produced white pocks rather than the red pocks of wt CPXV (Nathaniel et al., 2004; Pickup et al., 1984; Palumbo et al., 1994; Ray et al., 1992).

Interestingly, we found only a relatively small difference in the degree of pathogenesis associated with the wt CPXV and crmA-deficient CPXV (CPXVΔcrmA) when the two were compared following i.t. inoculation. However, differences between the two viruses were more obvious when the i.d. route was used. Specifically, CPXVΔcrmA infections led to a greater influx of $CD3^+$ mononuclear cells in the skin with elimination of the virus by 16 days post inoculation (dpi), whereas high amounts of wt CPXV could be isolated at this time point. We were also able to demonstrate that i.t. inoculation of C57BL/6 mice with CPXV resulted in viral pneumonia with a disease course analogous to smallpox in humans.

Results

Effect of crmA on the terminal caspase activity of CPXV-infected cultured cells

Previously, crmA was found to block apoptosis in CPXV-infected porcine cells (Ray and Pickup, 1996) presumably by inhibiting two initiators of this cell-death process, namely caspases-8 and -10 (Garcia-Calvo et al., 1998; Zhou et al., 1997). More recently, it was shown that CPXVΔcrmA, unlike wt CPXV, fails to inhibit apoptosis in infected chorioallantoic membranes of developing chicken embryos based on its inability to prevent activation of terminal caspases-3 and -7 (Nathaniel et al., 2004). To ensure that this deficiency of CPXVΔcrmA was attributed only to a genetic loss of the crmA gene, a rescue mutant (rCPXV) was derived from this recombinant and assessed for its ability to preclude apoptosis. The extent of cleavage of the caspase substrate Ac-DEVD-aminomethylcoumarin (AMC) in lysates of CPXV- and rCPXV-infected porcine renal epithelial (LLC-PK1) cells was similar to that achieved in uninfected cells (all less than 1 fluorescence unit/s). In contrast, a greater than 10-fold increase in caspase activity was detected in the CPXVΔcrmA-infected cells (19.15 fluorescence units/s). Thus, as expected, expression of crmA was sufficient for CPXV-directed inhibition of caspase activation and apoptosis in infected cells.

Effect of crmA on the virulence of CPXV intratracheally inoculated into mice

The reported lethal dose of half (LD50) of BALB/c mice after i.n. inoculation with CPXV is 2×10^5 plaque-forming units (pfu)/mouse (Thompson et al., 1993). In comparison, C57BL/6 mice were markedly more sensitive to i.t. inoculation of CPXV as the effective LD50 for these conditions was approximately 100-fold lower at 3.2×10^3 pfu/mouse. Accordingly, for assessing the effect of crmA on CPXV virulence *in vivo*, C57BL/6 mice were i.t.-inoculated with 10^4 pfu of CPXV, CPXVΔcrmA, or rCPXV and monitored for signs of distress. By 15 dpi, at least half of the CPXV- or rCPXV-infected mice were euthanized, whereas only approximately 20% of those inoculated with CPXVΔcrmA had to be terminated (Fig. 1). Moreover, the onset of disease signs such as weight loss, hunched posture, breathing difficulty, hypothermia, dependent edema, lethargy, poor grooming, abdominal distention, and (rarely) pock development on non-haired skin was more rapid and more pronounced in the CPXV- and rCPXV-

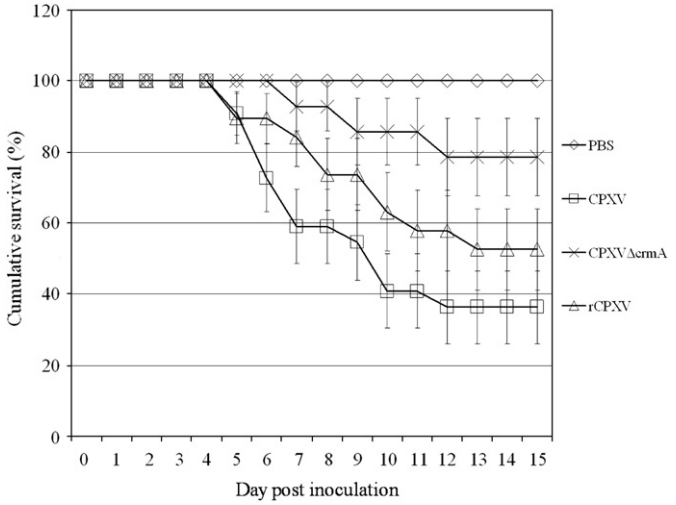

Fig. 1. Survival rate. Cumulative survival of C57BL/6 mice after i.t. inoculation of 30 μL PBS ($n=12$), 10^4 pfu CPXV ($n=22$), 10^4 pfu CPXVΔcrmA ($n=22$), or 10^4 pfu rCPXV ($n=19$). Results are the composite of three experiments. Error bars represent standard error.

infected mice than in the CPXVΔcrmA-treated mice. Thus, loss of crmA expression appeared to somewhat attenuate CPXV in C57BL/6 mice.

The pathology of intratracheal CPXV infections in mice and the effect of crmA

Cytological examination of bronchoalveolar lavage (BAL) fluid collected from the lungs of uninfected, CPXV-, and CPXVΔcrmA-infected C57BL/6 mice indicated an initial incidence of mild mononuclear inflammation in the lower respiratory tract at 1 dpi compared to 0.5 dpi. Since this event was a common feature in all experimental groups and the inflammation cleared by the second dpi, it probably represented a non-specific host response to the trauma of administration of 30 μL of fluid into the lungs. It was not until 9 to 11 dpi that a second round of inflammation was detected in BAL fluid of infected mice but not phosphate buffered saline (PBS)-inoculated mice. The severity of inflammation was similar both in CPXV- and CPXVΔcrmA-infected mice (data not shown).

Hematoxylin and eosin (H&E)-stained sections of lungs were evaluated for the presence of inflammation, hemorrhage, edema, necrosis, and fibrosis. Alterations were not observed in any lung samples obtained at 1 and 4 dpi. However by 7 dpi (Fig. 2) and thereafter, the majority of virus-infected mice had mild to moderate, multifocal, mixed (predominantly mononuclear) inflammation that tended to be focused around the bronchioles. The degree of bronchiolar epithelial hyperplasia and necrosis was moderate to severe with several bronchioles being affected. Generally, there was mild to moderate, multifocal, vascular necrosis and occasionally mild to moderate hemorrhage and edema (often associated with areas of vascular necrosis). Thus, the lesion characteristics were consistent with a diagnosis of moderate to severe viral bronchopneumonia characterized by mononuclear inflammation, bronchiolar hyperplasia, and necrosis.

As expected, due to differences in sample collection, inflammation was detected in the lung sections before it was observed in the BAL fluid. In both the sections of lung and the BAL fluid, the cellular characteristics of the inflammation observed were similar when comparing the lungs of mice infected with CPXV or CPXVΔcrmA. However, the severity of the lung lesions was slightly greater in animals infected with CPXV and this difference directly corresponded to the severity of clinical signs seen in these mice. Neither signs of disease nor histologic lesions were observed in the lungs of the control (PBS-inoculated) mice (Fig. 2).

Lesions were not observed in the brain of any mouse inoculated i.t. with PBS. In contrast, a mild focal lymphocytic infiltrate was noted in the cranial aspect of the brain in 1 mouse at 2 dpi and 1 mouse at 4 dpi from each of the CPXV and the CPXVΔcrmA experimental groups. A small lesion also was observed in 1 CPXVΔcrmA-infected mouse 7 dpi. The severity of clinical signs had no correlation to any brain lesions in either CPXV or CPXVΔcrmA i.t.-infected mice.

Tissue sections derived from heart, thymus, liver, spleen, kidney, gastrointestinal tract, and reproductive tract were unremarkable regardless of virus titer in the organ. On Day 7 post inoculation, 2 of 5 CPXV-infected animals had inflammation and necrosis in the nasal turbinates; viral inclusions were observed in secretory epithelial cells of 1 of these mice. Also, 1 of 5 CPXVΔcrmA-infected animals had mild hemorrhage in the epidermis and dermis of the nasal mucosa 7 dpi.

These findings indicate that i.t. inoculation of mice with 10^4 pfu of CPXV reproducibly causes bronchopneumonia, which is the cause of death in infected mice. The limited involvement of other organ systems (including brain and nasal mucosa) indicates that i.t. inoculation more accurately models smallpox pathogenesis than virus administered via the i.n. route. The effects of deleting the crmA gene on the pathology of the infection were detectable but minimal.

Effect of crmA on the virus replication in mice after intratracheal inoculation of CPXV

To determine the effects of deleting crmA on virus growth in mouse tissues, the virus titers within internal organs were determined from Day 0.5 through 15 post infection (Table 1). Tissues collected from i.t.-inoculated mice included lung, brain, liver, heart, spleen, kidney, intestine, and reproductive tract. Virus was detected in each of these organ systems, however only the lung and brain consistently contained detectable virus. Virus also was consistently recovered from BAL fluid collected from infected animals after euthanasia. Statistically significant differences in virus titer were not observed when comparing CPXV and CPXVΔcrmA infections. This indicates that deletion of crmA from CPXV does not affect the ability of the virus to replicate and spread after i.t. inoculation. Interestingly, increases in virus titer in tissue and BAL fluid samples did not correlate to an increase in clinical disease signs in the infected mice.

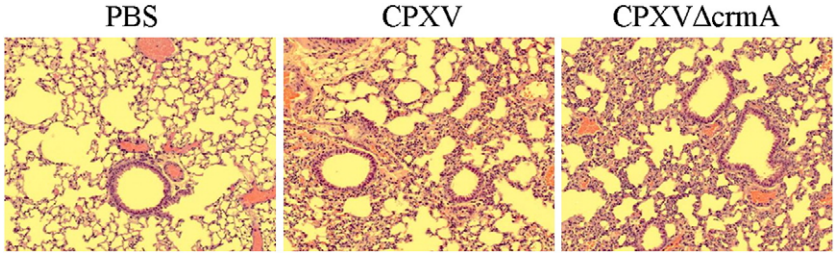

Fig. 2. Histopathology of lung sections. Representative lung sections from mice 7 d after i.t. inoculation with 30 μL PBS, 10^4 pfu CPXV, or 10^4 pfu CPXVΔcrmA (H&E; 200× magnification).

Table 1
Average virus titer from organs after intratracheal inoculation of mice[a]

	Days post inoculation[b]									
	1		4		7		11		15	
	CPXV	CPXV ΔcrmA	CPXV	CPXV ΔcrmA	CPXV	CPXV ΔcrmA	CPXV	CPXV ΔcrmA	CPXV	CPXV ΔcrmA
Lung	4.1	<4.0	6.2	6.2	7.0	7.1	5.5	7.2	6.7	7.5
BAL	<4.0	<4.0	8.4	7.3	7.0	7.6	7.3	7.9	6.2	5.0
Brain	nvi	nvi	4.8	<4.0	5.6	5.3	6.2	<4.0	<4.0	<4.0
Liver	nvi	nvi	nvi	nvi	4.8	<4.0	nd	nd	nd	nd
Heart	nvi	nvi	nvi	nvi	nvi	<4.0	nd	nd	nd	nd
Spleen	nvi	nvi	nvi	nvi	<4.0	<4.0	nd	nd	nd	nd
Kidney	nvi	nvi	nvi	nvi	nvi	<4.0	nd	nd	nd	nd
Intestine	nvi	nvi	<4.0	nvi	nvi	nvi	nd	nd	nd	nd
Ovary	nvi	nvi	nvi	nvi	<4.0	4.0	nvi	nvi	<4.0	<4.0

Abbreviations: BAL = bronchoalveolar lavage fluid; nvi = no virus isolated; nd = not determined.
[a] C57BL/6 mice were inoculated intratracheally with 30 μL of PBS containing 10^4 plaque-forming units (pfu) of the indicated virus. Organs were collected at necropsy, flash-frozen in liquid nitrogen, and then stored at −80 °C until virus titers were determined. Four to ten mice were used for each experimental group.
[b] The virus titer isolated from the indicated organs is represented as the logarithm of the average pfu per gram of tissue. Virus was isolated from at least one mouse per group in organs with virus titers <4.0, but the average titer for the group was less than the limit of detection for the assay (approximately 10,000 pfu per gram of tissue).

Effect of crmA on apoptosis of cells in lungs and mediastinal lymph nodes of mice after intratracheal inoculation of CPXV

Inhibition of apoptosis by crmA has been associated with increased CPXV replication in the chorioallantoic membranes of developing chicken embryos (Nathaniel et al., 2004). To determine if crmA negatively regulated apoptosis during CPXV infection of mice without impacting the efficiency of virus replication, terminal deoxynucleotidyl transferase mediated dUTP nick-end labeling (TUNEL) of lungs and mediastinal lymph nodes from CPXV- and CPXVΔcrmA-infected mice was performed. Evidence of cell death was seen in all necrotic regions of the lungs and greater quantities of TUNEL-positive cells were observed in the mediastinal lymph nodes that drained the necrotic lesions. Although apoptosis was more readily detected in tissue from the infected mice compared to PBS-inoculated animals, a significant difference in this parameter was not observed between mice infected with CPXV compared to CPXVΔcrmA-infected animals (data not shown).

Effect of crmA on the cytokine and chemokine response of mice to intratracheal inoculation with CPXV

A temporal comparison of the serum concentrations of 18 immunomodulators in mice during the 15-day period after i.t. inoculation with PBS, CPXV, or CPXVΔcrmA indicated that statistically significant changes occurred for only four of these immunomodulators; namely IL-6, IL-10, keratinocyte-derived chemokine (KC), and IL-1β. Immune mediators were quantified using a Mouse Cytokine 18-Plex Panel (Bio-Rad Laboratories Inc., Hercules, CA). As seen in Fig. 3A, the quantity of circulating IL-6 was approximately three-fold greater in CPXV-infected mice compared to PBS control animals at 7 dpi (P-value<0.0001) and at least two-fold greater compared to CPXVΔcrmA-inoculated mice at 7 dpi (P-value=0.0003) and 9 dpi (P-value=0.0022). A similar enhancement of the amount of IL-10 (approximately 3-fold) was noted in the CPXV-inoculated mice at 7 dpi (Fig. 3B) compared to PBS or CPXVΔcrmA-inoculated animals (P-values<0.0001). Fig. 3C graphs serum KC levels; at 7 dpi, KC was increased 2 to 3-fold in CPXV- and CPXVΔcrmA-infected mice compared to PBS controls (P-values<0.0001 and =0.0023, respectively). It is interesting to note that the levels of KC were increased in all mice at 0.5 dpi, which may reflect the inflammation observed in BAL samples at this time point. IL-1β was increased 10-fold in CPXV-infected mice at 0.5 dpi compared to PBS- and CPXVΔcrmA-inoculated animals (P-values≤0.0003). However the concentration of IL-1β in CPXV-infected mice at 0.5 dpi did not exceed levels of IL-1β in mock-infected animals at 7 or 15 dpi and so is unlikely to be physiologically significant (Fig. 3D). The systemic levels of the other 14 tested immunomodulators in sera remained fairly constant regardless of how the mice had been treated.

BAL samples also were tested using the Mouse Cytokine 18-Plex Panel in attempt to quantitate local levels of immunomodulators in pulmonary tissue. At 7 dpi, the relative quantities of IL-1α, IL-1β, macrophage inflammatory protein-1α (MIP-1α), and KC in the BAL fluid from the CPXV-infected mice was increased compared to that of PBS- or CPXVΔcrmA-inoculated animals, however none of these differences were found to be statistically significant (data not shown).

The levels of IL-1β, IL-18, IL-10, IL-6, and KC were determined in the lungs using standard enzyme-linked immunosorbant assays (ELISAs). Significant increases in IL-1β and IL-18 levels did not occur. The increase in IL-10 observed at 7 dpi in serum was not detected in lung. On Day 7 post inoculation, IL-6 levels in CPXV-infected mice were 5832 pg/g of tissue, which was significantly greater compared to mice inoculated with PBS (1081 pg/g, P-value=0.0041) or CPXVΔcrmA (1366 pg/g, P-value=0.0067). Likewise KC concentrations were significantly higher in CPXV-infected mice (880 pg/g) compared to mice inoculated with PBS (89 pg/g, P-value<0.0001) or CPXVΔcrmA (239 pg/g, P-value=0.0009).

Effect of crmA on the virulence of CPXV intradermally inoculated into mice

Although elimination of the crmA gene slightly attenuated the resultant recombinant CPXV when i.t.-inoculated into mice, an obvious cause for this loss of virulence (such as increased inflammation in the lungs, decreased apoptosis of infected cells in the lungs, or reduced virus replication) was not apparent. Therefore, in an attempt to discern an *in vivo* function for crmA, we introduced CPXV and CPXVΔcrmA into the ear pinnae by i.d. inoculation since dermal infections represent the natural route of infection with CPXV. An initial appraisal of the relationship between lesion severity and dose dependency indicated that the recombinant was somewhat attenuated at doses between 10^3 and 10^6 pfu/mouse (data not shown). Based on this assessment, subsequent experiments utilized inocula containing 10^5 pfu virus to ensure differentiation of the two viruses. At this dosage, as exemplified by the clinical scores presented in Table 2 and the appearance of the infected ear pinnae in Fig. 4, CPXVΔcrmA was less pathogenic than CPXV.

Fig. 4 depicts the lesions seen at 4, 8, and 12 dpi. Redness was observed in all infected mice at 4 dpi. The ear pinnae of CPXV- and rCPXV-infected mice are markedly red and swollen at 8 dpi; whereas ear pinnae are red, but not swollen, in CPXVΔcrmA-infected mice. On 12 dpi, ear pinnae of CPXV- and rCPXV-infected mice remain markedly

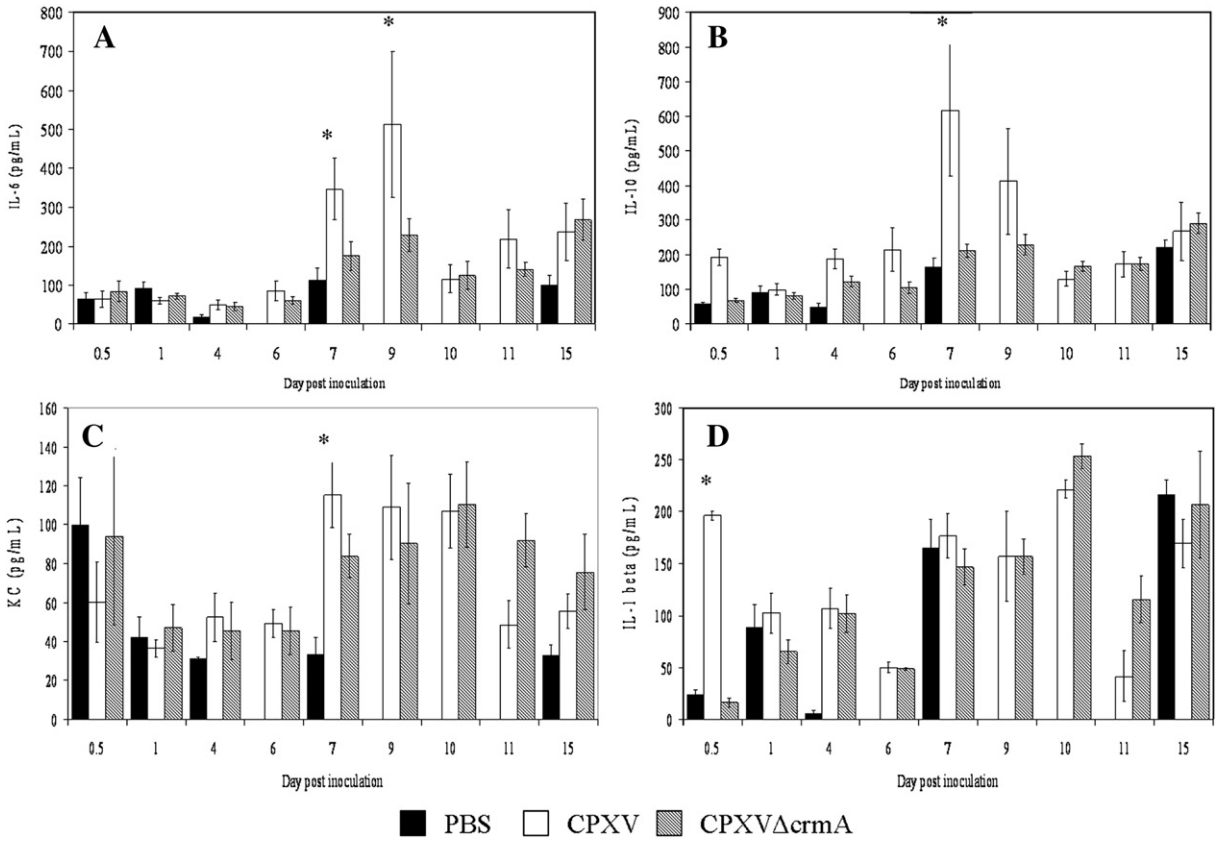

Fig. 3. Serum concentrations of immune mediators. Serum was collected at 0.5, 1, 4, 6, 7, 9, 10, 11, and 15 d after i.t. inoculation with 30 μL of 10^4 pfu CPXV or CPXVΔcrmA. The serum concentrations of these cytokines in uninfected mice were also detected at 0.5, 1, 4, 7, and 15 d after i.t. inoculation with 30 μL of PBS. Levels of immune mediators were detected using Mouse Cytokine 18-plex Panels. Serum IL-6 (A), IL-10 (B), KC (C), and IL-1β (D) levels are shown. Results of groups of 4 to 5 mice from 4 experiments were averaged. Error bars represent standard error of the mean. *Statistically significant differences (see text).

red and swollen (scabs also can be seen in the images); whereas CPXVΔcrmA-infected ear pinnae lesions have nearly resolved. Ear pinnae lesions from wt CPXV- and rCPXV-infected mice still were visible 15 dpi in approximately 60% of the inoculated mice and, in 2 cases, full-thickness tissue damage that led to loss of the infected ear pinnae occurred. Virus spread to secondary sites was observed at 12 dpi in 1 CPXV-infected mouse and 1 CPXVΔcrmA-infected mouse. However, signs of systemic illness (such as weight loss and poor grooming) were not noted in any experimental group (data not shown).

Effect of crmA on the histopathology observed in mice after intradermal inoculation of CPXV

Histological examination of ear pinnae from mice infected with either CPXV or CPXVΔcrmA revealed extensive edema and mononuclear inflammation with mild fibroblast reactivity at 4 dpi. Although dermal ulceration was observed in approximately two-thirds of the samples from either type of virus-infected mouse by 8 dpi, lesions were more severe in the pinnae from CPXV-inoculated animals. By 16 dpi, necrotizing lesions still persisted on 75% of CPXV-infected mice compared to only half of the CPXVΔcrmA-infected animals (data not shown).

Table 2
Gross pathology of ear pinnae after intradermal injection of mice[a]

	Days post inoculation[b,c]			
	4	8	12	15
CPXV	0.42 (59)	1.36 (50)	1.91 (32)	2.13 (23)
CPXVΔcrmA	0.44 (59)	0.96 (50)	1.19 (32)	0.83 (23)
rCPXV	0.67 (15)	1.97 (15)	1.87 (15)	2.27 (15)

[a] C57BL/6 mice were inoculated intradermally with 50 μL of PBS containing 10^5 plaque-forming units of the indicated virus.

[b] Pathogenesis represented by the average clinical score as determined by numerical assessment of the severity of lesions where 1=redness; 2=ulcers/scab; and 3=redness +ulcers/scab. Scores for treatment were summed and divided by the maximum, obtainable value (number of mice in group×3) to provide an average clinical score.

[c] The number of mice monitored at each timepoint is indicated in parentheses.

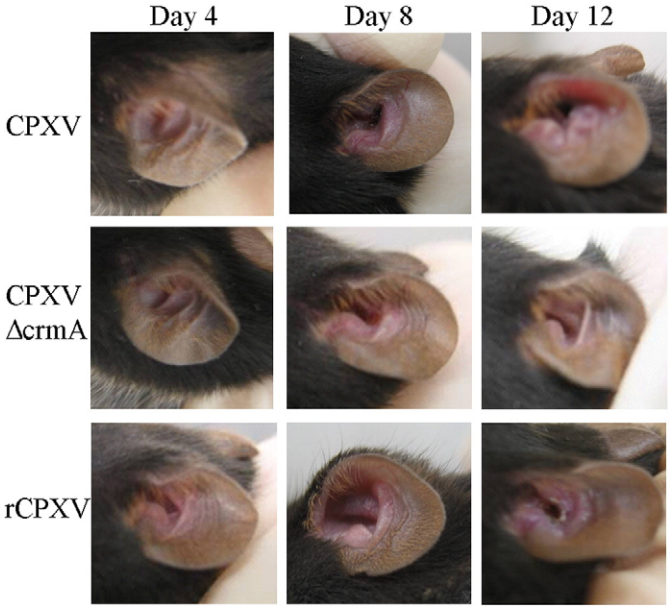

Fig. 4. Representative images of ear pinnae. Ear pinnae of C57BL/6 mice were infected i.d. with 10^5 pfu CPXV or CPXV recombinant viruses at 4, 8, and 12 dpi.

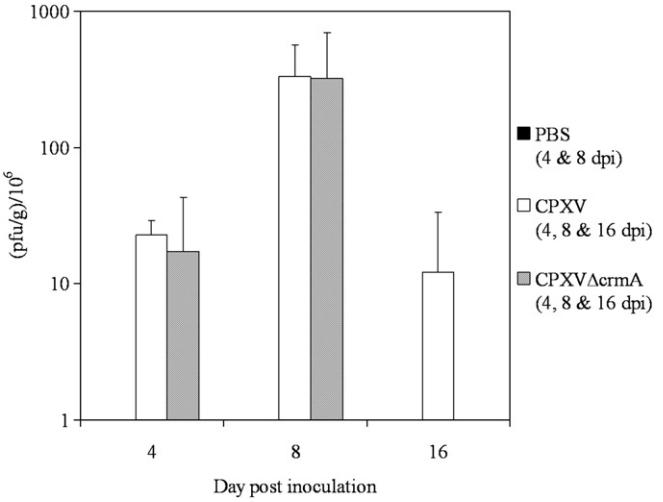

Fig. 5. Virus replication in the ear pinnae. The ears of mice were collected 4, 8, and 16 dpi with 50 μL PBS (right ear) and 10^5 pfu CPXV or CPXVΔcrmA (left ear). Results are presented as the average number of pfu per gram of ear pinnae (n=3 to 11 mice per group). Error bars represent standard deviation.

Effect of crmA on the virus replication in mice after intradermal inoculation of CPXV

Titration of infectious virus in ear pinnae samples from CPXV or CPXVΔcrmA i.d.-inoculated mice followed the pattern observed in the above-mentioned histological assessment. While a large amount of infectious virus was recovered from CPXV and CPXVΔcrmA-infected ears at 4 and 8 dpi, by 16 dpi only wt virus could be detected (Fig. 5). The enhanced clearance of CPXVΔcrmA could not be attributed to an increased number of apoptotic cells in the adjacent, draining lymphoid tissue as differences were not observed in the number of 7-amino-actinomycin D (7-AAD) positive cells by flow cytometry (data not shown).

Characterization of cell populations in lymphoid tissues of mice after intradermal infection

Cytokine levels were not examined in the i.d. mouse model due to lack of systemic disease signs. Instead, the phenotype of cells in various lymphoid tissues was evaluated. To determine if mice cleared i.d. infection with CPXVΔcrmA more quickly than with CPXV because of a more effective response by cytotoxic T cells, natural killer (NK) cells, or NKT cells; these cell populations were evaluated in the mandibular lymph nodes (which drain the ear pinnae), inguinal lymph nodes, and spleen.

As expected, given the lack of systemic disease, differences were not observed in the cell populations from the spleen or inguinal lymph nodes at any time point after PBS, CPXV, or CPXVΔcrmA inoculation. Interestingly, when compared to cell counts from PBS-inoculated mice, a relative increase in activated $CD4^+$ cells (3-fold or more), $CD8^+$ cells (4-fold or more), and NK cells (7-fold or more) was observed in mandibular lymph nodes of all infected mice; however statistical significance was not reached (data not shown).

Effect of crmA on the infiltration of $CD3^+$ mononuclear cells at the site of replication of CPXV intratracheally or intradermally inoculated into mice

One possible cause for the differential persistence of CPXV versus CPXVΔcrmA in ear pinnae as compared to a similar presence of both viruses in the lungs of infected mice would be disparities in number of anti-viral inflammatory cells infiltrating into these tissues. Although we were unable to discriminate between subpopulations of cytotoxic and antigen-presenting cells by immunohistochemical means, this process was successful for the overall identification of T cells based on their $CD3^+$ status. Accordingly, the mobilization of this type of cell into sites of CPXV infection was examined temporally (Fig. 6). No significant difference was observed in the number of $CD3^+$ mononuclear cells within the lungs of CPXV-infected mice compared to CPXVΔcrmA-infected mice at any time point (Fig. 6A). In contrast to the i.t.-inoculated mice, a significantly greater accumulation of $CD3^+$ cells was noted at the dermal site of CPXVΔcrmA replication as compared to that for the wt virus at 8 dpi (Fig. 6B). The increased number of $CD3^+$ cells associated with the CPXVΔcrmA infection may account for enhanced clearance of this virus 8 days later (Fig. 5).

Discussion

One of the goals of this work is to formally present and endorse the i.t. small animal respiratory model of Orthopoxvirus infection and to further emphasize the necessity to evaluate more than one model

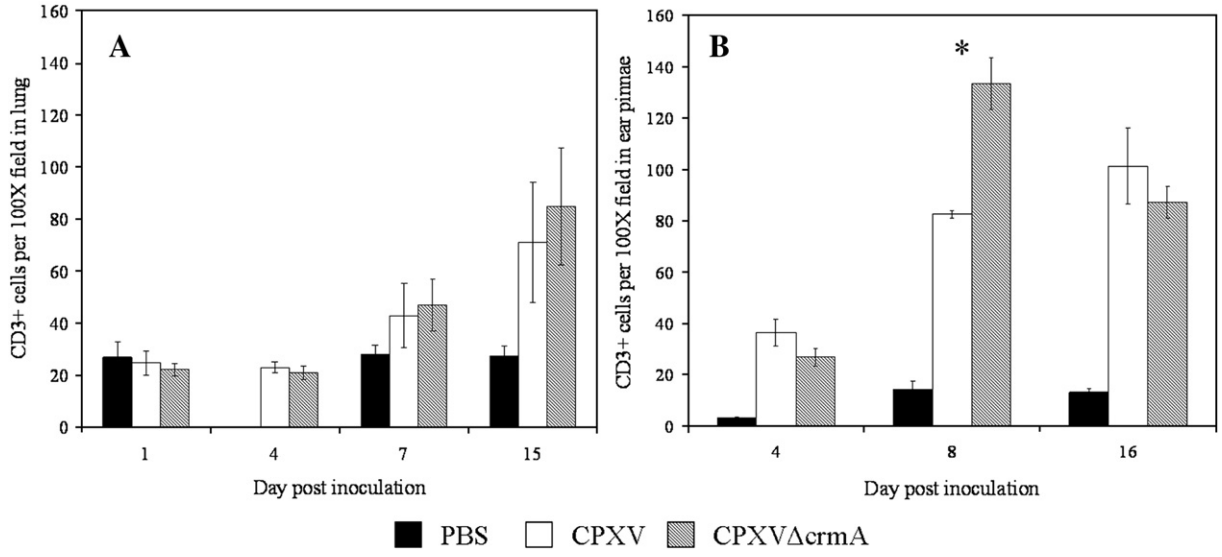

Fig. 6. Average number of $CD3^+$ cells per 100× magnified field in lesions of mouse lung (A) and ear pinnae (B) after inoculation with PBS, CPXV, or CPXVΔcrmA. Error bars represent standard error of the mean. *P-value of cells in CPXV- versus CPXVΔcrmA-infected mice=0.008.

when assessing the contribution of various virus-encoded immunomodulators or other virulence factors. The i.t. model of CPXV inoculation reproducibly caused lesions consistent with viral bronchopneumonia; these lesions are consistent with the terminal symptoms we observed and are the cause of death of infected mice. The inoculum volume that we used (30 μL) is approximately 18% of the mean tidal volume of a 5-week-old mouse (Fairchild, 1972) and was well tolerated with minimal signs of respiratory distress or reflux of fluid. Histological lesions in the lungs were evenly distributed among lung lobes which suggests that i.t. inoculation improves distribution of fluid throughout the lungs compared to i.n. administration. The i.t. route allows a precise dose of virus to be introduced into the respiratory tract with little involvement of the nasal cavity resulting in more animal to animal consistency. This procedure also greatly reduces or eliminates death due to rhinitis and sinusitis (which are often unintended sequelae of i.n. infection). Intratracheal inoculation also results in a lower dose of CPXV required to cause severe disease by 100-fold when compared to i.n. infections (3.2×10^3 pfu/mouse i.t. compared to 2×10^5 pfu/mouse i.n.). Hence we believe that the i.t. route of inoculation of mice with CPXV and other Orthopoxviruses provides an effective, sensitive, and reproducible model of pulmonary Orthopoxvirus infection and is superior to the i.n. model.

The somewhat increased survival rate and reduction of clinical signs observed in mice infected i.t. with CPXVΔcrmA compared to CPXV-infected mice indicate that crmA makes some contribution to virulence during pulmonary infection of C57BL/6 mice. Although survival data with rCPXV did not precisely equal results with wt CPXV, the differences were not statistically significant and clinical signs indicated the virulence of rCPXV and CPXV were similar. The increase in survival rate with CPXVΔcrmA agrees with overall results observed after i.n. infection with CPXV deleted for crmA in BALB/c mice (Thompson et al., 1993) and VACV deleted for SPI-2 (crmA) in BALB/c×C57BL/6 mice (Legrand et al., 2004). However, following i.t. inoculation, CPXVΔcrmA attenuation was modest and observable only within a narrow dose range; doses lower than 10^3 pfu/mouse did not cause significant disease signs in CPXV- or CPXVΔcrmA-infected mice and doses greater than 5×10^4 pfu/mouse caused severe disease in both experimental groups. This limited window of differential susceptibility may explain the lack of attenuation reported in studies with i.n. VACV deleted for SPI-2 in BALB/c mice (Kettle et al., 1995).

In the i.t. model, the severity of pulmonary inflammation correlated to severity of clinical symptoms but no quantitative differences were found in virus titer, number of apoptotic cells, or number of $CD3^+$ cells in lesions when CPXV- and CPXVΔcrmA-infected mice were compared. This finding is in contrast to a recent study showing that i.n. inoculation with the VACV Western Reserve (WR) strain causes slightly decreased numbers of $CD3^+$ mononuclear cells in the animals' lungs compared to infection with the attenuated Wyeth strain (Hayasaka et al., 2007); although this comparison should be made with caution given the fact that VACV Wyeth is known to be attenuated and contains several uncharacterized genetic mutations.

The i.d. route of infection using the ear pinnae as the site for introduction of virus was also examined in this study. Intradermal infection of mice with CPXVΔcrmA was attenuated compared to infection with CPXV, similar to what was observed during i.t. inoculation. Interestingly, i.d. infection with CPXV caused more severe inflammation at the site of inoculation throughout the time course of disease, but the number of infiltrating $CD3^+$ cells was decreased by 8 dpi compared to CPXVΔcrmA-infected mice. This result parallels that observed after i.n. inoculation of VACV WR and VACV Wyeth (Hayasaka et al., 2007). The increase in $CD3^+$ cells in the ear pinnae of animals infected with CPXVΔcrmA likely contributed to the more rapid clearance of virus in these mice compared to animals infected with CPXV. This finding strongly supports the use of more than one route of inoculation to determine the effects of deletion of various poxvirus genes.

Recent studies, which established i.d. inoculation of BALB/c mice as a model of poxvirus pathogenesis, showed that injection of 10^6 pfu VACV caused smaller primary lesions than CPXV or VACVΔSPI-2, indicating that VACVΔSPI-2 was not attenuated in this model (Tscharke et al., 2002). It was supposed that the increased inflammatory response observed after i.d. infection with VACVΔSPI-2 was due to the lack of SPI-2 inhibition of pro-inflammatory caspase-1. The opposing results in that study and ours may be due to the different mouse strains used, but differences between VACV and CPXV pathogenesis or differences in activity or specificity of the homologues SPI-2 and crmA must also be considered.

To further characterize the differences observed during i.t. CPXV and CPXVΔcrmA infection, we evaluated the effect of crmA deletion on cytokine levels to determine if crmA limited IL-1β and IL-18 processing. The mild increases observed in IL-1β and IL-18 levels were unlikely to be physiologically significant at any time point during infection with either CPXV or CPXVΔcrmA. This is consistent with the finding that i.n. inoculation with VACV deleted for SPI-2 did not cause IL-1β-induced fever but VACV deleted for the soluble IL-1β receptor did (Kettle et al., 1997). It is most likely that, even the absence of crmA, IL-1β and IL-18 levels are controlled by soluble IL-1β receptor, IL-18 binding protein, and other redundant immunomodulatory proteins encoded by CPXV and CPXVΔcrmA. Several additional cytokines and chemokines that are typically increased during inflammation were also maintained at low levels during CPXV and CPXVΔcrmA infection. CPXV encodes virulence proteins that could downregulate most of the mediators normally increased during an inflammatory process.

The cytokines and chemokines that were present at increased levels in sera of infected mice from 7 to 9 dpi were IL-6, IL-10, and KC. This agrees in part with Knorr et al. (2006) whom reported increases in serum IL-6, IL-10, and granulocyte/macrophage colony stimulating factor (GM-CSF) 6 days after i.n. inoculation of BALB/c mice with 3×10^5 pfu CPXV. However, we did not observe an increase in GM-CSF using the Bio-Rad Mouse Cytokine 18-plex Panel and the Panomics TranSignal Mouse Cytokine Antibody Array used by Knorr et al. (2006) does not detect KC. There are no known CPXV-encoded proteins that directly control levels of IL-6, IL-10, or KC. All three of these immunomodulators would be expected to be increased during severe virus-induced inflammation and necrosis. The relative increase in serum IL-6, IL-10, and KC during CPXV infection (compared to CPXVΔcrmA infection) is reflective of the more severe necrosis and inflammation caused by CPXV.

It is difficult to speculate why interleukin levels in lung homogenates did not parallel serum cytokine levels more precisely. Again, the relative increase in IL-6 and KC during CPXV infection compared to CPXVΔcrmA mirrors the disease severity observed with CPXV infection. However, the control of IL-10 in infected lungs cannot be explained by this line of thought. The flow-based multiplex bead array method has been compared to standard ELISAs; comparable patterns of cytokine levels were reported with both assays, however absolute values varied with the manufacturer of the assay (Khan et al., 2004).

Ultimately, the levels of all cytokines and chemokines tested were remarkably low, given the amount of inflammation observed in infected lungs, which indicates CPXV can control the levels of immune mediators present during infection. Interestingly, VACV is not able to prevent increases in interferon-γ (IFN-γ), tumor necrosis factor-α (TNF-α), nitric oxide, monocyte chemotactic protein-1 (MCP-1), MIP-1α, eotaxin, KC, or MIP-2 in BAL fluid during i.n. infection of BALB/c mice (Reading and Smith, 2003). This may indicate that CPXV immunomodulatory proteins are better adapted to inhibit the mouse immune system than VACV proteins; the larger genome size of CPXV compared to VACV likely contributes to the inherently increased immunomodulatory function of CPXV. However the mouse strain used may have made a significant difference in the host immune system response to virus infection. The minimal increase in all cytokines and chemokines tested also suggests that CPXV produces virulence factors

with redundant functions, since crmA deletion from CPXV did not disrupt control of the majority of immune mediators tested.

We were also unable to see any effect of crmA on the number of apoptotic cells in the lungs and mediastinal lymph nodes of i.t.-inoculated animals or in the mandibular lymph nodes draining the ear pinnae of i.d-inoculated animals. This result was surprising because crmA is necessary to control apoptosis in infected chicken chorioallantoic membranes (Nathaniel et al., 2004). However, embryonated chicken eggs have an intact innate immune response, but have not yet developed a cell-mediated immune response (Chen et al., 1994; Masteller et al., 1997). It is likely that control of apoptosis is not as critical in animal models with a rapid cell-mediated immune response, such as the mouse.

In conclusion, i.t. inoculation of 10^4 pfu CPXV in mice causes a reproducible severe pulmonary disease which mimics smallpox-induced pneumonia in humans. Deletion of crmA from CPXV caused some attenuation in the i.t. mouse pulmonary disease model and as well as after i.d. inoculation. In the both models, inflammation observed in H&E-stained tissue sections corresponded to the severity of disease signs and was not increased, as predicted, during CPXVΔcrmA infection. Virus growth was not significantly affected by crmA deletion after i.t. inoculation of virus, but it was cleared by 16 days after i.d. infection. An increase in the $CD3^+$ mononuclear cell population was seen in ear pinnae 8 dpi and likely contributed to the more rapid clearance of virus from mice infected with CPXVΔcrmA. The mechanism by which crmA inhibits infiltration of $CD3^+$ cells remains unclear. It would be interesting to determine whether crmA mediates small changes in cytokine levels at the site of an i.d. infection which limit infiltration of $CD3^+$ cells and allow prolonged virus replication to occur.

Materials and methods

Cells and viruses

African green monkey kidney (CV-1) fibroblasts and LLC-PK1 cells were obtained from the American Type Culture Collection (ATTC CCL-70 and CL-101 respectively). CV-1 cells were maintained in minimum essential medium (MEM) with Earle's salts and LLC-PK1 cells in medium 199 (GIBCO, Grand Island, NY), both supplemented with 5% fetal bovine serum (GIBCO), 2 mM glutamine, 50 U/mL penicillin G, 50 μg/mL streptomycin, 1 mM sodium pyruvate, and 0.1 mM nonessential amino acids (Mediatech, Herndon, VA) and incubated at 37 °C in a 5% CO2 atmosphere with 100% humidity. Three viruses were used in this study: the wild type Brighton Red strain of cowpox virus (CPXV) was obtained from David Pickup (Duke University Medical Center, Durham, NC, U.S.A.); a crmA-deficient derivative of CPXV (CPXVΔcrmA) [originally designated CPVΔcrmA::lacZ (Nathaniel et al., 2004)]; and a rescue mutant (rCPXV). Rescued CPXV was generated from CPXVΔcrmA in the following manner. First, a 1682 bp region encompassing the crmA ORF and approximately 300 nucleotides of upstream and downstream flanking DNA was amplified from the CPXV genome by using forward primer FS1 (GGTTCGGTGGCAAACTTTCCATGG), reverse primer FS43 (CGCGAACGTCGATGAACACTGATTCCGCATC), and Vent polymerase (New England Biolabs, Ipswich, MA). After confirmation of its nucleotide sequence, 2 μg of the amplicon were transfected in the presence of Lipofectamine (Invitrogen, Carlsbad, CA) and 1 μg of CPXVΔcrmA DNA into CV-1 cells previously inoculated for 1 h with CPXVΔcrmA at a multiplicity of infection (moi) of 0.05. Progeny were screened for insertion of the crmA gene based on their inability to hydrolyze 5-bromo-4-chloro-3-indolyl-D-galactoside (X-gal) present in media added to the agarose overlays of infected CV-1 monolayers. After four rounds of plaque-purification, the rCPXV was passed once in CV-1 monolayers. The insertion of the crmA ORF into the genome of the rescue virus was verified by nucleotide sequence analysis of the relevant region and the use of immunoblotting to demonstrate the presence of crmA in the lysate of infected CV-1 cells as described previously (Nathaniel et al., 2004).

Terminal caspase activity assays

Monolayers of LLC-PK1 cells were mock-treated or infected at a moi of 10 with CPXV, CPXVΔcrmA, or rCPXV. At 15 hpi, the cells were harvested, concentrated by centrifugation at 2000 ×*g* for 10 min at 4 °C, and resuspended in 100 μL 10 mM HEPES pH 7.5, 2 mM EDTA, 0.1% CHAPS, and 1 mM DTT. The cell suspension was frozen/thawed 4 times and clarified at 5000 ×*g* for 15 min at 4 °C. Terminal caspase activity in 5 μg of protein was measured as previously described (Nathaniel et al., 2004). The rates of cleavage observed in four independent infections with each virus were averaged and compared to the average rate of cleavage from four mock-treated (uninfected) cells.

Intratracheal inoculation of mice

Groups of five or more 5-week-old female C57BL/6 specific-pathogen-free (spf) mice (The Jackson Laboratory, Bar Harbor, ME) were infected with sequential 10-fold dilutions of CPXV or CPXVΔcrmA from 10^5 to 10^3 pfu of virus to determine the effective lethal dose of 50% of the mice (eLD50). This parameter is defined as the quantity of virus that would cause sufficiently severe respiratory distress in half of the respective infected mice to necessitate their euthanasia and was calculated according to the Reed and Muench formula (Reed and Muench, 1938). The largest difference between the eLD50s of CPXV and CPXVΔcrmA was observed at a dose of 10^4 pfu/mouse, so this dose was chosen for the remainder of the experiments. Three experimental groups of mice were combined to obtain survival rates after infection. Four additional experimental groups were used for organ histopathology and cytokine levels in BAL fluid and blood. Two of the experimental groups were used to collect lung for ELISAs over a time course of infection. Two experimental groups were used for virus isolation from organs. The number of mice used for each experiment with each virus and each time point varied from 3 to 10 mice per group.

For all experiments, mice were anesthetized with isoflurane gas or by intraperitoneal (i.p.) injection of a combination of 80 to 90 mg/kg ketamine HCl and 12 to 15 mg/kg xylazine diluted in sterile isotonic sodium chloride. The mice were placed in a supine position and the skin at the ventral aspect of the throat was surgically prepared. A 0.5 cm incision was made on the ventral aspect of the throat and a sterile microchip that transmitted a numeric identification for each mouse along with body temperature (BioMedic Data Systems, Inc., Seaford, DE) was inserted under the skin to the left of the thorax over the pectoral muscles. The trachea was carefully exposed by blunt dissection and 30 μL of diluted virus or PBS was injected i.t. through a 30 gauge needle. The surgical wound was closed with either a sterile surgical clip or sterile tissue glue. Animals were monitored twice a day for up to 23 days.

For non-survival experiments, at the appropriate times post inoculation, animals were anesthetized as described above. The axial artery was severed with scissors to collect blood then mice were euthanized by i.p. injection of 150 mg/kg sodium pentobarbital (Schering-Plough Animal Health, Union, NJ). A BAL sample was collected at the time of death and a complete necropsy was preformed. Organs were placed in 10% buffered formalin (Protocol; Fisher Scientific, Kalamazoo, MI) for histopathological examination and immunohistochemical analysis or they were flash-frozen in liquid nitrogen for virus isolation and evaluation of cytokine levels by ELISA.

Intradermal inoculation of mice

Three to five 5-week-old female C57BL/6 spf mice were infected i.d. in their left ear pinnea with 50 μL of PBS containing sequential 10-fold

dilutions from 10^6 to 10^2 pfu of either CPXV, CPXVΔcrmA, or rCPXV. The largest difference in CPXV and CPXVΔcrmA pathogenesis was observed at 10^5 pfu/mouse. Therefore, for subsequent experiments, each animal received 10^5 pfu virus i.d. In all cases, the left ear pinna of each mouse was infected with virus while the right ear was injected with PBS to serve as a negative control site. Gross pathology of ear pinnae were scored based on the following numerical system: 1=redness; 2=ulcers/scab; and 3=redness+ulcers/scab. Scores for treatment were summed and divided by the maximum, obtainable value (number of mice in group×3) to provide an average clinical score. A separate control group of mice that did not receive any virus, but were injected with PBS in both ears, were included for experiments that utilized flow cytometry to identify cell subsets in lymph nodes.

Prior to i.d. inoculation, the mice were anesthetized with isoflurane gas and their ear pinnae wiped with 70% ethanol. The ear pinna were then gently extended away from the head and PBS containing or lacking virus was injected at the base of the left or right ear, respectively, between the dorsal and ventral aspects of the pinna using a 30 gauge needle. Animals were monitored twice a day for up to 26 days.

At the appropriate times post inoculation, mice were euthanized as described above. Ear pinnae were removed and placed in 10% buffered formalin (Protocol; Fisher Scientific) for future histopathological analysis (n=9 per group) or flash-frozen for later virus titration (n=3 to 11 mice per group). Spleen, mandibular lymph nodes, and inguinal lymph nodes were collected for cell identification by flow cytometric analysis and cytology or for histopathology. Samples from three mice were pooled to ensure enough cells were recovered for flow cytometry. The lymphoid organs were diced in PBS using two 30 gauge needles. The resulting cell suspension was filtered through a 70 μm Nylon membrane (BD Biosciences, Bedford, MA) into 50 mL conical tubes. Flow cytometry results from three sets of experimental groups were averaged.

Virus isolation from mice

Tissue collected from animals was flash-frozen in liquid nitrogen and stored at −80 °C until they were processed. Tissues were weighed and 1 mL of PBS was added to each sample. The samples were disrupted using a MiniBeadbeater-8 (BioSpec Products, Inc., Bartlesville, OK), diluted 1:100 in media without serum, and sonicated. Monolayers of CV-1 cells were inoculated with serial dilutions of the organ samples and plaque assays were performed to determine virus titer.

TUNEL of apoptotic cells from CPXV-infected mice

The ApopTag Apoptosis Detection Kit (Chemicon International, Inc., Temecula, CA) was used to perform TUNEL assays on deparaffinized sections of lung and mediastinal lymph nodes of C57BL/6 mice i.t.-infected with 30 μL PBS alone or containing 10^4 pfu of CPXV or CPXVΔcrmA. Samples were stained following the manufacturer's protocol. Upon completion of the procedure, the sectioned tissue was stored in the dark at −20 °C until analyzed during the subsequent 12 h by fluorescent microscopy.

Determination of chemokine and cytokine levels in serum and BAL samples

Sera and BAL fluid were collected from C57BL/6 mice infected i.t. with 30 μL PBS alone or containing 10^4 pfu of CPXV or CPXVΔcrmA. Levels of eighteen chemokines and cytokines [IL-1α, IL-1β, IL-2, IL-3, IL-4, IL-5, IL-6, IL-10, IL-12 subunit p40, IL-12 subunit p70, IL-17, IFN-γ, TNF-α, MIP-1α (CCL3), the regulation on activation normal T expressed and secreted protein (RANTES, CCL5), KC (Gro-1, Gro-α, CXCL1), granulocyte colony stimulating factor (G-CSF), and GM-CSF] were quantified in each sample by using the Mouse Cytokine 18-plex Panel in a Bio-Plex Multi-Plex Cytokine Assay (Bio-Rad Laboratories) according to manufacturer's instructions for pre-mixed multiple assays. A Bio-Plex Diluent Kit for mouse serum samples was used as directed to dilute serum samples (1:4) and kit standards. BAL samples were not diluted. Standards for BAL samples were diluted in PBS.

Determination of chemokine and cytokine levels in lung tissue

Liquid nitrogen-frozen samples of lung tissue from i.t.-inoculated C57BL/6 mice were placed into 17×100 mm centrifuge tubes (Corning, Inc., Acton, MA) and 5 weight-volumes of cold PBS was added to each sample (n=4 to 5 mice per experimental group). Samples were homogenized for 1 min with a Polytron homogenizer (Glen Mills Inc., Clifton, NJ) then centrifuged for 10 min at 4 °C and 10,000 rpm (Beckman J2-H5). The supernatant was collected and stored at −80 °C until assayed for the presence of IL-1β, IL-18, IL-6, IL-10, and KC by the use of commercially available ELISAs.

Identification of cell subsets in lymphoid tissues

Samples collected for cytology and flow cytometry were centrifuged at 400 ×g and 4 °C for 5 min. The supernatant was removed and cell pellets from inguinal lymph node samples were resuspended in cold Hanks azide buffer (HAB) adjusted to pH 7.4 [Hanks balanced salt solution without Ca^{2+} or Mg^{2+} (JRH Biosciences, Inc., Lenexa, KS), 1% bovine serum albumin, 0.1% NaN_3, 1 mM EDTA]. Cell pellets from the spleen and mandibular lymph nodes were first resuspended in 0.84% NH_4Cl for 5 min on ice to lyse red blood cells, centrifuged as above, and then resuspended in cold HAB. The number of cells collected from each sample was determined using a hemocytometer.

Approximately 2×10^6 cells from each sample were placed in 12×75 mm polystyrene tubes (Fisher Scientific Co., Pittsburg, PA) for flow cytometry. Cells were washed in HAB, centrifuged as above, and then resuspended in 100 μL 4% HAB (HAB plus an additional 3% bovine serum albumin) and 2 μL Mouse Fc Block (BD Biosciences, San Jose, CA). These samples were incubated in the dark for 10 min at RT. The appropriate fluorescent dye-conjugated monoclonal antibodies (mAb; BD Biosciences) were added to each tube. Samples were incubated with the antibodies in the dark at RT for 15 min. Cells were pelleted as above and finally resuspended in 500 μL HAB and 5 μL 7-AAD (BD Biosciences).

Flow cytometry was performed using a FACSCalibur four color analyzer (BD Biosciences). BD CellQuest Pro Software for Mac OSX was used to acquire and analyze the flow cytometry data. To establish flow cytometric parameters, splenocytes were incubated with isotype controls for each antibody. Splenocytes also were incubated with rat anti-mouse CD8a mAbs conjugated to the appropriate fluorochromes (BD Biosciences) to compensate for overlap of emission wavelengths detected by the flow cytometer. The total number of $CD4^+$ cells (helper T cells), $CD8^+$ cells (cytotoxic T cells), natural killer (NK, $NK1.1^+/CD49b^+$) cells, and NKT ($NK1.1^+/CD3^+$) cells was determined for each experimental group at 4, 8, and 16 dpi. Activation of these cells, excluding NKT cells, also was determined. Analysis of activated $CD4^+$ and $CD8^+$ cells was done by identifying the cells in these subsets that were double positive for CD25 and CD69. The number of activated NK cells was determined from the number of $CD25^+$ cells that were also $NK1.1^+$. Data from each cell type examined (except apoptotic cells) were gated on cell size to remove cell fragments and on 7-AAD. 7-AAD positive cells were considered dead cells and were not included in the analysis. Apoptotic helper and cytotoxic T cells were analyzed using Annexin-V-FITC (Apoptosis Detection Kit I, BD Biosciences). As a positive control for apoptosis, 100 μM staurosporine (Sigma Chemical, St.

Louis, MO) was added to 2×10^6 lymphoid cells from PBS-inoculated mice for 4 h prior to incubation of the cells with Mouse Fc Block. Staurosporine-treated cells were then processed as described above.

Identification of CD3+ cells in the lungs and ear pinnae

Staining of $CD3^+$ cells in sections of formalin-fixed lungs from C57BL/6 mice i.t.-inoculated with PBS alone or 10^4 pfu CPXV or CPXVΔcrmA or ear pinnae from animals i.d. injected with PBS or 10^5 pfu of virus was performed by the Histopathology Section of the Veterinary Diagnostic Laboratory at the University of Illinois (Urbana, IL). Cells reactive with a rabbit polyclonal anti-human CD3 antibody (Dako, Carpinteria, CA) were identified by using light microscopy (100× magnification).

Statistics

Survival data was analyzed using PROC GENMOD in SAS 9.1 to perform a logistic regression of the data. Analysis of differences in virus titers, cytokine levels, and number of lymphocyte subsets was conducted using a mixed model analysis program, PROC MIXED, in SAS 9.1. The ability to isolate virus after infection with CPXV or CPXVΔcrmA was compared using a Fisher's exact test. The numbers of $CD3^+$ cells in infected tissues was evaluated by ANOVA using MedCalc version 9.5.1.0.

Acknowledgments

We are indebted to members of the Department of Statistics at the University of Florida who analyzed the majority of quantitative data presented in this manuscript. We would like to thank David Tscharke and Geoff Smith for their helpful instruction with the ear pinnae model. A special thank you goes to William Schnitzlein and Gail Sherba for their help in editing this manuscript. This research was funded primarily by the National Institute of Health (grants AI-15722, R56 AI-15722, and DE-07200) and in part by University of Illinois start-up funds.

References

Breman, J.G., Henderson, D.A., 2002. Diagnosis and management of smallpox. N. Engl. J. Med. 346, 1300–1308.
Chantrey, J., Meyer, H., Baxby, D., Begon, M., Bown, K.J., Hazel, S.M., et al., 1999. Cowpox: reservoir hosts and geographic range. Epidemiol. Infect. 122, 455–460.
Chen, C.H., Gobel, T.W., Kubota, T., Cooper, M.D., 1994. T cell development in the chicken. Poult. Sci. 73, 1012–1018.
Dieli, F., Lio, D., Sireci, G., Salerno, A., 1988. Genetic control of C3 production by the S region of the mouse MHC. J. Immunogenet. 15, 339–343.
Fairchild, G.A., 1972. Measurement of respiratory volume for virus retention studies in mice. Appl. Microbiol. 24, 812–818.
Fenner, F., 1984. Smallpox, "the most dreadful scourge of the human species." Its global spread and recent eradication. Med. J. Aust. 141, 841–846.
Ferrier-Rembert, A., Drillien, R., Tournier, J.N., Garin, D., Crance, J.M., 2007. Intranasal cowpox virus infection of the mouse as a model for preclinical evaluation of smallpox vaccines. Vaccine 25, 4809–4817.
Garcia-Calvo, M., Peterson, E.P., Leiting, B., Ruel, R., Nicholson, D.W., Thornberry, N.A., 1998. Inhibition of human caspases by peptide-based and macromolecular inhibitors. J. Biol. Chem. 273, 32608–32613.
Hawranek, T., Tritscher, M., Muss, W.H., Jecel, J., Nowotny, N., Kolodziejek, J., et al., 2003. Feline orthopoxvirus infection transmitted from cat to human. J. Am. Acad. Dermatol. 49, 513–518.
Hayasaka, D., Ennis, F.A., Terajima, M., 2007. Pathogeneses of respiratory infections with virulent and attenuated vaccinia viruses. Virol. J. 4, 22.
Janeway, C.A., Travers, P., Walport, M., Capra, J.D., 1999. Immunobiology. Garland Publishing, New York.
Kettle, S., Blake, N.W., Law, K.M., Smith, G.L., 1995. Vaccinia virus serpins B13R (SPI-2) and B22R (SPI-1) encode M(r) 38.5 and 40K, intracellular polypeptides that do not affect virus virulence in a murine intranasal model. Virology 206, 136–147.
Kettle, S., Alcami, A., Khanna, A., Ehret, R., Jassoy, C., Smith, G.L., 1997. Vaccinia virus serpin B13R (SPI-2) inhibits interleukin-1 beta-converting enzyme and protects virus-infected cells from TNF- and fas-mediated apoptosis, but does not prevent IL-1 beta-induced fever. J. Gen. Virol. 78, 677–685.
Khan, S.S., Smith, M.S., Reda, D., Suffredini, A.F., McCoy Jr., J.P., 2004. Multiplex bead array assays for detection of soluble cytokines: comparisons of sensitivity and quantitative values among kits from multiple manufacturers. Cytometry B Clin. Cytom. 61, 35–39.
Knorr, C.W., Allen, S.D., Torres, A.R., Smee, D.F., 2006. Effects of cidofovir treatment on cytokine induction in murine models of cowpox and vaccinia virus infection. Antivir. Res. 72, 125–133.
Legrand, F.A., Verardi, P.H., Jones, L.A., Chan, K.S., Peng, Y., Yilma, T.D., 2004. Induction of potent humoral and cell-mediated immune responses by attenuated vaccinia virus vectors with deleted serpin genes. J. Virol. 78, 2770–2779.
Lewis-Jones, S., 2004. Zoonotic poxvirus infections in humans. Curr. Opin. Infect. Dis. 17, 81–89.
Martin, D.B., 2002. The cause of death in smallpox: an examination of the pathology record. Mil. Med. 167, 546–551.
Martinez, M.J., Bray, M.P., Huggins, J.W., 2000. A mouse model of aerosol-transmitted orthopoxviral disease — morphology of experimental aerosol-transmitted orthopoxviral disease in a cowpox virus-BALB/c mouse system. Arch. Pathol. Lab. Med. 124, 362–377.
Masteller, E.L., Pharr, G.T., Funk, P.E., Thompson, C.B., 1997. Avian B cell development. Int. Rev. Immunol. 15, 185–206.
Melamed, S., Paran, N., Katz, L., Ben-Nathan, D., Israely, T., Schneider, P., Lenin, R., Lustig, S., 2007. Tail scarification with vaccinia virus lister as a model for evaluation of smallpox vaccine potency in mice. Vaccine 25, 7743–7753.
Nathaniel, R., MacNeill, A.L., Wang, Y.X., Turner, P.C., Moyer, R.W., 2004. Cowpox virus CrmA, myxoma virus SERP2 and baculovirus P35 are not functionally interchangeable caspase inhibitors in poxvirus infections. J. Gen. Virol. 85, 1267–1278.
Nitsche, A., Gelderblom, H.R., Eisendle, K., Romani, N., Pauli, G., 2007. Pitfalls in diagnosing human poxvirus infections. J. Clin. Virol. 38, 165–168.
Palumbo, G.J., Buller, R.M., Glasgow, W.C., 1994. Multigenic evasion of inflammation by poxviruses. J. Virol. 68, 1737–1749.
Pickup, D.J., Ink, B.S., Parsons, B.L., Hu, W., Joklik, W.K., 1984. Spontaneous deletions and duplications of sequences in the genome of cowpox virus. Proc. Natl. Acad. Sci. U. S. A. 81, 6817–6821.
Quan, L.T., Caputo, A., Bleackley, R.C., Pickup, D.J., Salvesen, G.S., 1995. Granzyme B is inhibited by the cowpox virus serpin cytokine response modifier A. J. Biol. Chem. 270, 10377–10379.
Ray, C.A., Pickup, D.J., 1996. The mode of death of pig kidney cells infected with cowpox virus is governed by the expression of the crmA gene. Virology 217, 384–391.
Ray, C.A., Black, R.A., Kronheim, S.R., Greenstreet, T.A., Sleath, P.R., Salvesen, G.S., et al., 1992. Viral inhibition of inflammation: cowpox virus encodes an inhibitor of the interleukin-1 beta converting enzyme. Cell 69, 597–604.
Reading, P.C., Smith, G.L., 2003. A kinetic analysis of immune mediators in the lungs of mice infected with vaccinia virus and comparison with intradermal infection. J. Gen. Virol. 84, 1973–1983.
Reed, L.T., Muench, H.A., 1938. A simple method of estimating fifty percent endpoints. Am. J. Hyg. 27, 493–497.
Smith, G.L., Howard, S.T., Chan, Y.S., 1989. Vaccinia virus encodes a family of genes with homology to serine proteinase inhibitors. J. Gen. Virol. 70 (Pt 9), 2333–2343.
Thompson, J.P., Turner, P.C., Ali, A.N., Crenshaw, B.C., Moyer, R.W., 1993. The effects of serpin gene mutations on the distinctive pathobiology of cowpox and rabbitpox virus following intranasal inoculation of Balb/c mice. Virology 197, 328–338.
Tscharke, D.C., Reading, P.C., Smith, G.L., 2002. Dermal infection with vaccinia virus reveals roles for virus proteins not seen using other inoculation routes. J. Gen. Virol. 83, 1977–1986.
Zhou, Q., Snipas, S., Orth, K., Muzio, M., Dixit, V.M., Salvesen, G.S., 1997. Target protease specificity of the viral serpin CrmA — analysis of five caspases. J. Biol. Chem. 272, 7797–7800.